Available online at www.sciencedirect.com
SCIENCE DIRECT®
Optics Communications 223 (2003) 417–423
OPTICS COMMUNICATIONS
www.elsevier.com/locate/optcom

Simultaneous amplitude modulation and wavelength conversion in an asymmetric-duty-cycle periodically poled lithium niobate

Y.H. Chen [a,*], F.C. Fan [a], Y.Y. Lin [a], Y.C. Huang [a], J.T. Shy [b], Y.P. Lan [c], Y.F. Chen [c]

[a] Department of Electrical Engineering, National Tsing-Hua University, Hsinchu 300, Taiwan, ROC
[b] Department of Physics, National Tsing-Hua University, Hsinchu 300, Taiwan, ROC
[c] Department of Electro-physics, National Chiaotung University, Hsinchu 300, Taiwan, ROC

Received 17 October 2002; received in revised form 19 June 2003; accepted 19 June 2003

Abstract

We report the theory and experiment for an amplitude modulator and wavelength converter based on an electrode-coated asymmetric-duty-cycle periodically poled lithium niobate (PPLN). In a 56%/44% domain-duty-cycle PPLN crystal, we modulated the amplitude of the 532-nm second-harmonic output and measured a normalized half-wave voltage of 1.1 V $\times$ d (μm)$/l_{\mathrm{eff}}$ (cm), where d is the separation of the electrodes and l_{eff} is the effective electrode length defined by the PPLN length multiplying the deviation of the domain-duty-cycle from the 50% value. A modulation depth of 85% was obtained in the linear modulation regime. We also derived a unified theory to describe the half-wave voltage for two types of PPLN-based amplitude modulators.

PACS: 42.65.Ky; 42.55.−f

Keywords: Laser; Nonlinear optics; Wavelength conversion; Amplitude modulation

1. Introduction

Periodically poled lithium niobate (PPLN) is a popular nonlinear crystal employing the quasi-phase-matching (QPM) technique [1]. A PPLN crystal has several desirable advantages such as having a large effective nonlinear coefficient, wide transparent range, and long available crystal length. The QPM technique alters the sign of the nonlinear coefficient every coherence length in a nonlinear optical material. This periodic sign reversal also occurs to the electro-optic coefficient in the material. Recently, electro-optic wavelength tuning in PPLN by applying an electric field to either the $+z$ or $-z$ domains has been proposed [2]. Although, according to [2], the electric field is

* Corresponding author. Tel.: +886-3-5741066; fax: +886-3-5741067.
E-mail address: yehchen@mx.nthu.edu.tw (Y.H. Chen).

0030-4018/$ - see front matter
doi:10.1016/S0030-4018(03)01674-2

expected to penetrate throughout the whole ferroelectric domain under the electrode, our finite-element computer simulation showed a uniform, unmodulated field profile in the crystallographic x–y plane for a depth deeper than the PPLN grating period. For example, in a 30-μm period PPLN, the periodic field profile only exists approximately 30-μm from the PPLN surface. A more feasible electro-optic wavelength tuning technique is to use an electrode-coated asymmetric-duty-cycle PPLN, which has been demonstrated experimentally in an optical parametric oscillator with reduced nonlinear conversion efficiency [3]. While wavelength tuning is important for laser applications, laser amplitude modulation is often required for information transmission and high-resolution detection. The same principle used in [3] can be employed for simultaneous amplitude modulation and wavelength conversion at a resonance wavelength. A conceptual design of an amplitude modulator based on an asymmetric-duty-cycle QPM waveguide was proposed in 1993 [4]; however, the theoretical study was limited to a specific electrode configuration for a given domain inversion geometry in the waveguide. In this paper, we demonstrate the experiment and derive the complete theory for simultaneous amplitude modulation and wavelength conversion based on a general configuration of an electrode-coated asymmetric-duty-cycle PPLN crystal. We also compare this type of modulator with the segmented PPLN modulator [5,6] and provide a unified theory to describe the half-wave voltage for both devices.

2. Theoretical derivations

Without losing generality, we model the theory by using an example of second harmonic generation (SHG) in an electrode-coated asymmetric-duty-cycle PPLN crystal. The same technique can be applied to other phase-sensitive nonlinear optical processes. In the following, we first derive the theory in the low-efficiency regime and extend the result to the high-conversion limit.

In a material, the phasor of the electric field of the mixing wave i propagating in the x direction in a nonlinear material can be expressed by

$$E_i = A_i \mathrm{e}^{\mathrm{i}k_i \int_0^x n_i(x')\,\mathrm{d}x'}, \tag{1}$$

where A_i is a slowly varying field envelope along x, $k_i = 2\pi/\lambda_i$ is the vacuum wave number, and $n_i(x')$ is the refractive index at the longitudinal position $x = x'$. Throughout this paper, the subscript i is replaced by ω for the quantity associated with the fundamental wave and 2ω for that associated with the second harmonic wave, where ω is the angular frequency of the fundamental wave. Substituting Eq. (1) into the Helmholtz equation with second-order nonlinear polarization [7] and applying the slowly varying-envelope approximation, one has the governing equation for the SHG field envelope in a loss-less medium

$$\frac{\mathrm{d}A_{2\omega}}{\mathrm{d}x} + \frac{1}{2n_{2\omega}(x)}\frac{\mathrm{d}n_{2\omega}(x)}{\mathrm{d}x}A_{2\omega} = \Gamma d_{33}(x)\mathrm{e}^{-\mathrm{i}\int_0^x \Delta k(x')\,\mathrm{d}x'}, \tag{2}$$

where $\Delta k(x') = k_{2\omega}\Delta n(x') = k_{2\omega}[n_{2\omega}(x') - n_{\omega}(x')]$ is the wave vector mismatch, $\Gamma \equiv (i16\pi^2/n_{2\omega}(x)\lambda_{\omega})A_{\omega}^2$ is the coupling coefficient, and $d_{33}(x)$ is the relevant nonlinear coefficient in a PPLN crystal. When an electric field E_z is applied to the PPLN crystal in the crystallographic c direction, the refractive index experienced by wave i is modified by the electric field according to

$$n_{\pm,i}(E_z) = n_{\mathrm{e},i} \pm r_{33,i}n_{\mathrm{e},i}^3 E_z/2, \tag{3}$$

where the choice of sign depends on the polarization of the ferroelectric domain, n_e is the extraordinary refractive index, and r_{33} is the Pockels coefficient. In the following the subscript + or − depends on the choice of n_+ or n_- in the calculation.

To obtain the second harmonic field at the PPLN output, one may integrate Eq. (2) over x with the assumption of low conversion efficiency and thus a constant fundamental power. Fig. 1 illustrates one period of the PPLN crystal that

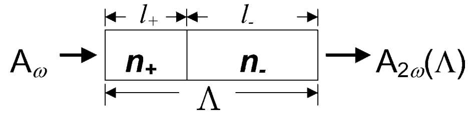

Fig. 1. The schematic of a crystal period in an asymmetric-duty-cycle PPLN. The crystal period consists of two unequal-length crystal domains with opposite ferroelectric polarizations.

consists of two unequal domain lengths, l_+ and l_-, with the PPLN grating period of $\Lambda = l_+ + l_-$.

By integrating Eq. (2), the second harmonic field generated from such a PPLN period $A_{2\omega}(\Lambda)$ is given by

$$A_{2\omega}(\Lambda) = id_{33}\left(\Gamma_+ \frac{e^{-i\Delta k_+ l_+} - 1}{\Delta k_+} - \Gamma_- \frac{e^{-i\Delta k_- l_-} - 1}{\Delta k_-} e^{-i\Delta k_+ l_+}\right), \quad (4)$$

where according to Eq. (3), the wave vector mismatch $\Delta k_\pm$ can be further expressed by

$$\Delta k_\pm = \Delta k_0 \pm \delta k = \frac{2\pi}{\lambda_{2\omega}}\left[(n_{e,2\omega} - n_{e,\omega}) \pm \left(\frac{1}{2} r_{33,2\omega} n^3_{e,2\omega} - \frac{1}{2} r_{33,\omega} n^3_{e,\omega}\right) E_z\right]. \quad (5)$$

Assume that the PPLN crystal consists of N periods, having a length of $L = N \times \Lambda$. To calculate the SHG field envelope after N periods, one may integrate Eq. (2) directly to obtain

$$A_{2\omega}(N\Lambda) = A_{2\omega}(\Lambda) \times \sum_{n=1}^{N} e^{-i(n-1)(\Delta k_+ l_+ + \Delta k_- l_-)} = A_{2\omega}(\Lambda) \times \frac{\sin\left[N\left(\Delta k_+ \frac{D\Lambda}{2} + \Delta k_- \frac{(1-D)\Lambda}{2}\right)\right]}{\sin\left(\Delta k_+ \frac{D\Lambda}{2} + \Delta k_- \frac{(1-D)\Lambda}{2}\right)} \times \exp -i(N-1)\left(\Delta k_+ \frac{D\Lambda}{2} + \Delta k_- \frac{(1-D)\Lambda}{2}\right), \quad (6)$$

where $D \equiv l_+/\Lambda$ is the PPLN domain-duty-cycle. In integrating each QPM domain, the second term on the left-hand side of Eq. (2) was eliminated, since the refractive index remained constant in the range of integration. Eq. (6) is similar to the far field expression of a diffraction grating with N periods, as the total SHG field is coherently summed up from each crystal period. The SHG output intensity after N periods is therefore

$$I_{2\omega}(N\Lambda) = I_{2\omega}(\Lambda) \frac{\sin^2\left[N\left(\Delta k_+ \frac{D\Lambda}{2} + \Delta k_- \frac{(1-D)\Lambda}{2}\right)\right]}{\sin^2\left(\Delta k_+ \frac{D\Lambda}{2} + \Delta k_- \frac{(1-D)\Lambda}{2}\right)} = I_{2\omega}(\Lambda) \frac{\sin^2(\delta k \times l_{eff})}{\sin^2(\delta k \times \delta\Lambda)}, \quad (7)$$

where $I_{2\omega}(\Lambda)$ is the SHG intensity generated from one PPLN period, $\delta\Lambda \equiv |D - 1/2| \times \Lambda$ is the effective electrode length in each PPLN period, and $l_{eff} \equiv N \times \delta\Lambda = |D - 1/2| \times L$ is the effective electrode length over the whole PPLN crystal. Usually N is a large number. For instance, a 2-cm PPLN crystal for frequency doubling 1064 nm laser through the third-order QPM process has approximately a thousand periods. As a result, the sinc-like term, $\sin^2(\delta k \times l_{eff})/\sin^2(\delta k \times \delta\Lambda)$, is much more sensitive to the applied electric field than $I_{2\omega}(\Lambda)$. For $D = 1/2$ and $E_z \neq 0$, the grating term is no longer a function of the electric field and this device in practice can not be used as an amplitude modulator. For $D = 1/2$ and $E_z = 0$, Eq. (7) is reduced to the expected expression for a standard PPLN SHG device [8], given by

$$I_{2\omega}(L) = \left(\frac{\Gamma 2 d_{33}}{\pi} L\right)^2 \bigg/ 2\eta, \quad (8)$$

with the first-order QPM phase matching condition $\Delta k = 2\pi/\Lambda$, where η is the wave impedance.

Although Eq. (7) does not have the typical sinusoidal expression for most electro-optic modulators, one may define the half-wave voltage to be the one that is required to vary Eq. (7) from its maximum value to its first zero, corresponding to a voltage that changes the phase $\delta k \times l_{eff}$ by π. With the help of Eq. (5), the half-wave voltage has the familiar form

$$V_\pi = \frac{d}{(D - 1/2)L} \frac{\lambda_{2\omega}}{(r_{33,2\omega} n^3_{e,2\omega} - r_{33,\omega} n^3_{e,\omega})} = \frac{d}{l_{eff}} \frac{\lambda_{2\omega}}{(r_{33,2\omega} n^3_{e,2\omega} - r_{33,\omega} n^3_{e,\omega})}, \quad (9)$$

where d is the separation of the two electrodes, $r_{33,i}$ is the electro-optic coefficient pertaining to wave i, and $n_{e,i}$ is the extraordinary refractive index seen by the wave i. It is seen that at a 50% domain-duty-cycle, Eq. (9) is no longer valid and the half-wave voltage is impractically large, governed by the term $I_{2\omega}(\Lambda)$.

For the first-order QPM process, nonlinear conversion efficiency decreases when the domain-duty-cycle deviates from the 50% value. However, in the blue and green spectrum, first-order PPLN periods are usually small and difficult to fabricate.

As a result, the third-order QPM process, having a grating period three times that for the first-order QPM process, is often the choice of frequency conversion involving mixing wavelengths comparable or shorter than 500 nm. For the third-order QPM SHG process, the conversion efficiency for $D = 1/2$ is the same as that for $D = 1/6$ or 5/6 [8]. Therefore choosing the domain-duty-cycle $D = 1/6$ or 5/6 allows the very QPM wavelength converter to function simultaneously as an amplitude modulator without sacrificing nonlinear frequency conversion efficiency, if the third-order QPM process has to be used. Fig. 2 plots Eq. (7) as a function of the electric field E_z for frequency doubling 1064 nm laser in a 45 mm long and 500 μm thick third-order PPLN crystal with $D = 1/6$ or 5/6, $n_{e,2\omega} = 2.2369$, $n_{e,\omega} = 2.17583$, $r_{33,2\omega} = 30.9$ pm/V, and $r_{33,\omega} = 29.4$ pm/V. The half-wave voltage is about 360 V or 1.1 (V cm/μm) $\times d$ (μm)$/l_{\mathrm{eff}}$ (cm), where d is the separation of the electrodes. For a waveguide device of a few centimeters in length, the electrode separation is on the order of 10 μm and the half-wave voltage can be less than 10 V.

For certain applications, it is important to choose the modulation point in the sinc-like curve. In Eq. (5), the E_z-dependent wave vector mismatch

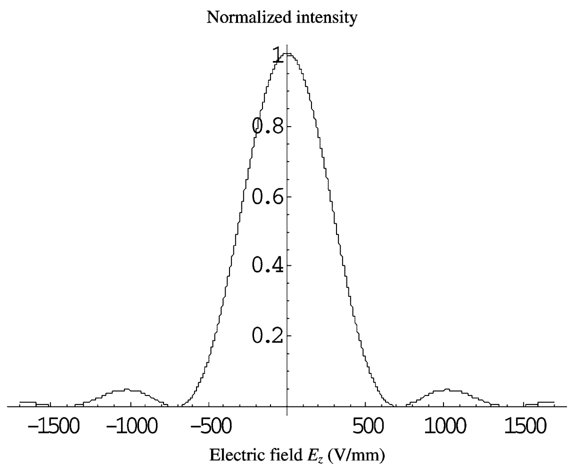

Fig. 2. The calculated SHG intensity versus the electric field E_z for frequency doubling 1064 nm laser in a 45 mm long and 500 μm thick third-order PPLN crystal with $D = 1/6$ or 5/6, $n_{e,2\omega} = 2.2369$, $n_{e,\omega} = 2.17583$, $r_{33,2\omega} = 30.9$ pm/V, and $r_{33,\omega} = 29.4$ pm/V. The half-wave voltage is about 360 V.

$$\delta k = \frac{2\pi}{\lambda_{2\omega}}\left[\left(\frac{1}{2}r_{33,2\omega}n_{e,2\omega}^3 - \frac{1}{2}r_{33,\omega}n_{e,\omega}^3\right)E_z\right], \tag{10}$$

is a function of temperature. Because the term $I_2(\Lambda)$ is relatively insensitive to temperature compared to the sinc-like grating term, one may simply adjust the PPLN crystal temperature to select the modulation point along the grating curve $\sin^2(\delta k \times l_{\mathrm{eff}})/\sin^2(\delta k \times \delta\Lambda)$.

It is instructive to compare the asymmetric-domain-duty-cycle PPLN modulator with the segmented PPLN modulator demonstrated by Chang et al. [9]. Fig. 3 depicts the schematic of the segmented PPLN modulator, wherein an electrode-coated lithium niobate section is sandwiched between two symmetric PPLN sections. In the low-conversion limit, the SHG output intensity is a result of the interference between the two SHG fields, $E_{2\omega,1}$ and $E_{2\omega,2}$, from the first and second PPLN sections, given by

$$I_{2\omega} = 4I_{2\omega,1}\cos^2(\Delta k l_d/2), \tag{11}$$

where

$$\Delta k = \frac{2\pi}{\lambda_{2\omega}}\left[(n_{e,2\omega} - n_{e,\omega}) + \left(\frac{1}{2}r_{33,2\omega}n_{e,2\omega}^3 - \frac{1}{2}r_{33,\omega}n_{e,\omega}^3\right)E_z\right],$$

is the phase mismatch in the dispersion region and $I_{2\omega,1} \equiv ((2d_{33}\Gamma/\pi m)\sin(\pi m D))^2\mathrm{sinc}^2(\Delta k_m l/2)$ is the SHG intensity generated from the first or the second PPLN crystal section under the mth-order QPM phase matching condition

$$\Delta k_m = \frac{2\pi}{\lambda_{2\omega}}[(n_{e,2\omega} - n_{e,\omega})] - \frac{2\pi m}{\Lambda}.$$

From (11), the half-wave voltage is given by

$$V_\pi = \frac{d}{l}\frac{\lambda_{2\omega}}{\left(r_{33,2\omega}n_{e,2\omega}^3 - r_{33,\omega}n_{e,\omega}^3\right)}, \tag{12}$$

which has the same form as that for an asymmetric-duty-cycle PPLN modulator, except that the latter has an effective electrode length of $l_{\mathrm{eff}} = (D - 1/2)L$.

Since Δk and Δk_m in Eq. (11) are both temperature dependent, it is usually difficult to select the modulation point by varying the temperature in a

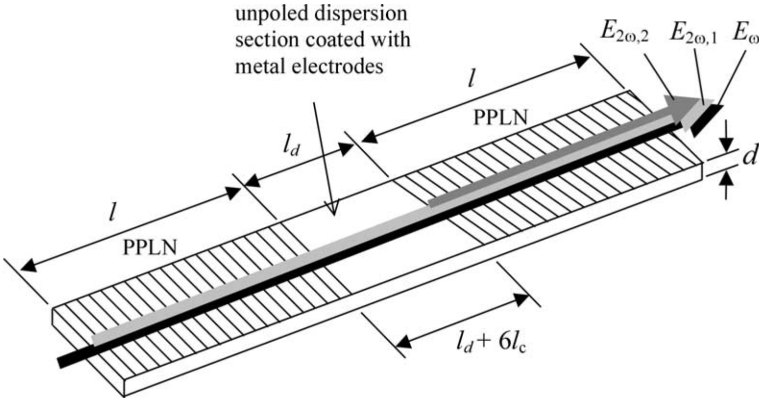

Fig. 3. The segmented PPLN modulator in [9], where a dispersion lithium niobate section is sandwiched between two symmetric PPLN sections. The length of the dispersion section varies from l_d to $l_d + 6l_c$, where l_c is the coherence length.

segmented PPLN modulator. As a result, Chang et al. fabricated the device in Fig. 3 with an adjustable dispersion length so as to select the modulation point. In addition, any asymmetry existing in the two PPLN crystal sections could influence the spatial coherence between $E_{2\omega,1}$ and $E_{2\omega,2}$, and decrease the modulation depth of this device [5]. On the other hand, the asymmetric-duty-cycle modulator has no such an issue.

The previous analysis was based on a low-conversion-efficiency assumption. In the high-conversion regime, the power of the fundamental wave also varies with distance and the exact value of the local SHG field has to be solved iteratively from a full set of coupled-wave Eq. (10). To understand the behavior of such a device in the high-conversion limit, we numerically solved the couple-wave equations for frequency doubling a 1064-nm laser in a first-order PPLN crystal with a 40%/60% domain-duty-cycle. The PPLN crystal has a 10-mm length and 500-μm thickness. In the simulation, we injected different pump powers to obtain 34%, 84%, and 94% peak efficiencies under the perfect phase matching condition and then started to apply an external voltage to vary the SHG efficiencies. Fig. 4 shows the calculated SHG conversion efficiency as a function of the electrode voltage for different peak efficiencies. When a voltage is applied to this device, the QPM phase matching condition is detuned and the shape of the curves in Fig. 4 is similar to that with the detuning Δk in the abscissa [10,11]. Therefore, it is not surprising that the high-efficiency curve in Fig. 4 looks like a Jacobi elliptic function and the low-efficiency curve in the same plot remains a sinc function. Due to the narrow acceptance bandwidth in the high-conversion limit, the half-wave voltage decreases about 10 times when the conversion efficiency varies from 34% to 94%.

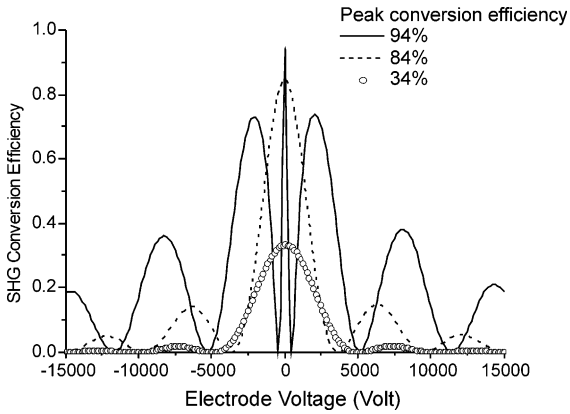

Fig. 4. The calculated SHG conversion efficiency versus the electrode voltage for frequency doubling 1064-nm laser in a first-order PPLN crystal with a 40%/60% domain-duty-cycle. The PPLN crystal has a 10-mm length and 500-μm thickness. Due to the narrow acceptance bandwidth in the high-conversion limit, the half-wave voltage decreases about 10 times when the peak conversion efficiency varies from 34% to 94%.

3. A proof-of-principle experiment

To conduct a proof-of-principle experiment, we fabricated a third-order PPLN crystal for frequency doubling a 1064-nm wavelength laser. The PPLN has a grating period of 20.4 μm, a length of 45 mm, and a thickness of 0.5 mm. In general, it is difficult to control the domain-duty-cycle in the PPLN fabrication process. With an available photomask for fabricating ~50% domain-duty-cycle PPLN, we deliberately over poled the lithium niobate crystal in the electric field poling process to obtain a 56%/44% duty-cycle PPLN crystal. The domain-duty-cycle was calculated by averaging the domain lengths under a microscope. We pumped the electrode-coated PPLN with a 300 mW $Nd:YVO_4$ laser and generated a maximum power of 1.5 mW at the 532 nm wavelength.

Fig. 5 shows the SHG temperature tuning-curves with voltages of −1.2, 0, +1.2 kV applied to the PPLN crystal. It is evident from the figure that the electric field indeed altered the SHG output power. The temperature tuning 0.5 °C/kV is consistent with the theoretical value calculated from the Sellmeier equation and Eq. (7) for $D = 56\%$. Clearly, one may choose the modulation point on the sinc-like curve simply by varying the temperature.

Fig. 6 shows the SHG output power versus the applied voltage at 36.5 °C. Due to the voltage limit of our power supply, we only traced out a portion of the sinc-like curve in Eq. (7). Nonetheless, it clearly shows a half-wave voltage of ~2 kV, which is in good agreement with the normalized half-wave voltage 1.1 (V cm/μm) × d (μm)/l_{eff} (cm) predicted in theory, if one takes into account the 4.5 cm crystal length, the 0.5-mm crystal thickness, and the $D = 56\%$ domain-duty-cycle.

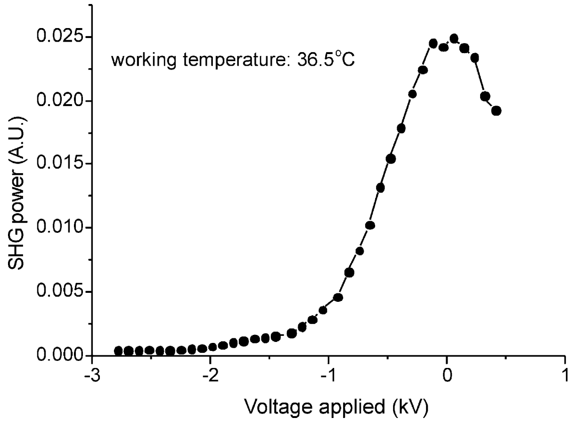

Fig. 6. A ~2 kV half-wave voltage was measured for the 45 mm long, 0.5 mm thick, 56%/44% domain-duty-cycle PPLN modulator, which is consistent with the theoretical prediction.

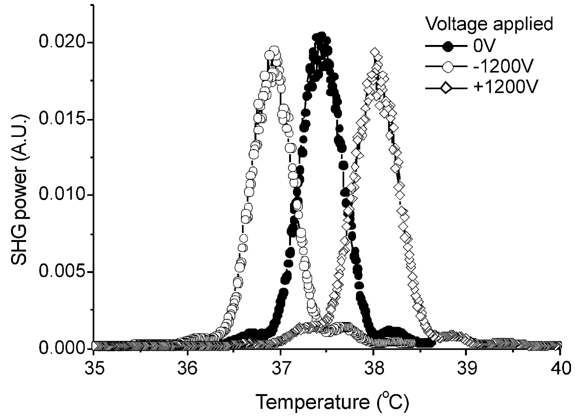

Fig. 5. The SHG temperature tuning-curves with voltages of −1.2, 0, +1.2 kV applied to the PPLN crystal. The temperature tuning 0.5 °C/kV is consistent with the theoretical value calculated from the Sellmeier equation and Eq. (7) for $D = 56\%$.

Fig. 7 shows the modulated SHG signal with a modulation depth of 85% when a 600 V peak-to-peak, 200 Hz voltage was applied to the electrodes. To achieve linear modulation in Fig. 7, the modulation point was chosen by setting the crystal temperature ±0.35 °C from the phase-matching temperature.

4. Summary

We have demonstrated the feasibility of simultaneous amplitude modulation and second harmonic generation in an asymmetric-duty-cycle PPLN crystal. We also derived the theory that fully characterizes this device. We measured a normalized half-wave voltage of 1.1 (V cm/μm)× d (μm)/l_{eff} (cm) from a third-order SHG PPLN crystal, which is in good agreement with the theory. We also derived a unified theory for the half-wave voltage for the asymmetric-duty-cycle and the segmented PPLN modulators [5,9]. Compared to a segmented PPLN modulator, an asymmetric-

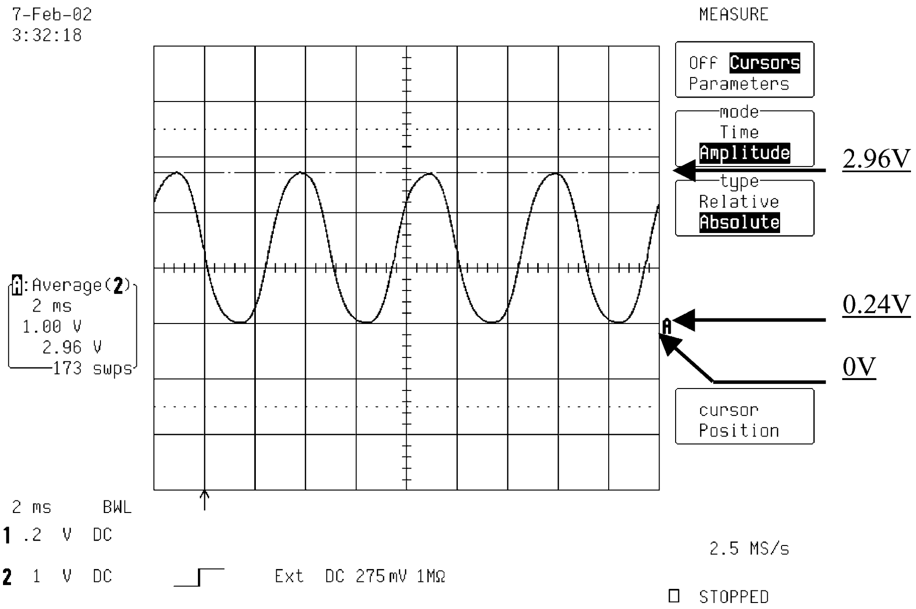

Fig. 7. The modulated SHG signal with a modulation depth of 85% when a 600 V peak-to-peak, 200 Hz voltage was applied to the electrodes. Linear modulation was achieved by setting the crystal temperature ±0.35 °C from the phase-matching temperature.

duty-cycle PPLN modulator has the advantage of a better modulation depth and the ease of choosing modulation point through temperature. For high-order QPM processes, it is possible to achieve amplitude modulation in an asymmetric-duty-cycle PPLN crystal without sacrificing nonlinear conversion efficiency, although it is in general difficult to fabricate a PPLN with a specified domain-duty-cycle. To achieve simultaneous amplitude modulation and wavelength conversion, the same technique described in this paper can be applied to other phase sensitive nonlinear optical processes, including sum frequency generation, different frequency generation, and optical parametric generation. This technique is particularly important for applications involving both wavelength conversion and information transmission. For example, optical communication and laser trace-gas sensing are among possible applications.

Acknowledgements

This work was supported by National Science Council, Taiwan, under Grant No. NSC 89-2622-L-007-007 and HC Photonics Inc. under NTHU Project 91A0128J6. Y.H. Chen's email address is yehchen@mx.nthu.edu.tw.

References

[1] J.A. Armstrong, N. Bloemergen, J. Ducuing, P.S. Pershan, Phys. Rev. 127 (1962) 1918.
[2] Y.Q. Lu, J.J. Zheng, Y.L. Lu, N.B. Ming, Appl. Phys. Lett. 74 (1999) 123.
[3] N. O'Brien, M. Missey, P. Powers, V. Dominic, Opt. Lett. 24 (1999) 1750.
[4] S. Helmfrid, K. Tatsuno, K. Ito, J. Opt. Soc. Am. B 10 (1993) 459.
[5] Y.C. Huang, K.W. Chang, Y.H. Chen, A.C. Chiang, T.C. Lin, B.C. Wong, J. Lightwave Technol. 20 (2002) 1165.
[6] S. Kurimura, Y. Uesu, Jpn. J. Appl. Phys. 33 (1994) 5457.
[7] R.W. Boyd, Nonlinear Optics, Academic Press, San Diego, 1992.
[8] M.M. Fejer, G.A. Magel, D.H. Jundt, R.L. Byer, IEEE J. Quan. Elec. 28 (1992) 2631.
[9] K.W. Chang, A.C. Chiang, T.C. Lin, B.C. Wong, Y.H. Chen, Y.C. Huang, Opt. Commun. 203 (2002) 163.
[10] R.C. Eckardt, J. Reintjes, IEEE J. Quan. Elec. QE-20 (1984) 1178.
[11] K.R. Parameswaran, J.R. Kurz, R.V. Roussev, M.M. Fejer, Opt. Lett. 27 (2002) 43.